

# Aluminum-doped Zinc Oxide Nanoparticles Sensing Properties Enhanced by Ultraviolet Light

Short paper

Sandrine Bernardini<sup>1</sup>, Tomas Fiorido<sup>1</sup>,  
Khalifa Aguir<sup>1</sup>

<sup>1</sup> Aix Marseille Univ, Univ Toulon, CNRS, IM2NP,  
Marseille, France  
e-mail: sandrine.bernardini@im2np.fr  
e-mail: tomas.fiorido@im2np.fr  
e-mail: khalifa.aguir@im2np.fr

Meriem Gaceur<sup>2</sup>, Olivier Margeat<sup>2</sup>, Jörg  
Ackermann<sup>2</sup>, Christine Vidélot-Ackermann<sup>2</sup>

<sup>2</sup> Aix Marseille Univ, CNRS, CINaM, Marseille, France  
e-mail: gaceur@cinam.univ-mrs.fr  
e-mail: margeat@cinam.univ-mrs.fr  
e-mail: ackermann@cinam.univ-mrs.fr  
e-mail: videlot@cinam.univ-mrs.fr

**Abstract** — The development of room-temperature gas sensors for nitrogen dioxide gases is of great importance for air quality monitoring due to unhealthy impact on human life and environment. In this work, we focus on Aluminum-doped Zinc Oxide sensing properties. We compare nitrogen dioxide detection at room temperature in dark and under ultraviolet or blue illuminations. Working temperature from 25°C up to 100°C have been also performed in dark and under UV and blue Light Emitted Diodes. Aluminum-doped Zinc Oxide nanoparticles have been deposited by drop coating from colloidal solution as sensitive layer for air quality monitoring on Si/SiO<sub>2</sub> substrate. Herein, a brief description of the process steps will be provided. We demonstrate that UV light and temperature enhance gas-sensing properties with good reversibility and repeatability.

**Keywords**-Gas sensor; NO<sub>2</sub> sensor; light excitation; Al-ZnO nanoparticles; Ultraviolet illumination; blue illumination.

## I. INTRODUCTION

Nitrogen dioxide (NO<sub>2</sub>) comes from vehicles, power plants, industrial emissions and off-road sources, such as construction, lawn and gardening equipment. It is one of the most dangerous air pollutants. It plays a major role in the formation of ozone and acid rain. Continued or frequent exposure to NO<sub>2</sub> concentrations higher than 0.15 ppm may cause incidence of acute respiratory. To detect NO<sub>2</sub>, resistive gas sensors are the most attractive due to easy fabrication, simple operation, low production cost and miniaturization. Zinc oxide (ZnO) is a wide band gap (about 3.37 eV at room temperature) II-IV n-type semiconductor that has many applications. It is one of the best candidates for air quality monitoring having large accessibility for the targeted gases. Moreover, doping is one possible way to improve the sensibility of the ZnO nanoparticles (NPs). ZnO is usually doped with small amounts of metal ions, such as Al, Ga, etc. We have recently reported our preliminary work on room temperature NO<sub>2</sub> detection achieved by Aluminum-doped Zinc Oxide (Al-ZnO) sensitive layer on Si/SiO<sub>2</sub> substrate enhanced by UltraViolet (UV) light [1]. Al-ZnO can be produced as nanoparticles and keep the same advantages as ZnO NPs in terms of layer

processing. However, its conductivity can be three orders of magnitudes higher [2]. Operating at room temperature is interesting for working in explosive environment and also with flexible substrate to fit any shape needed on smart objects. In literature, several technics have been described to decrease the operating temperature and improve the sensitivity and stability of metal oxide (MOX) gas sensors, such as noble metal doping [3], transition metal oxide incorporation [4-5], light activation [6-8]. Among them, adding UV light at ZnO surface is the most studied to achieve room temperature sensitivity [9-12].

Recently, Prof. Zhang's team has reported that visible light illumination can greatly enhance the NO<sub>2</sub> sensing performance of sensors performed with solution precursor plasma spray (SPPS) of n-n heterojunctions formed between SnO<sub>1-α</sub>, ZnO<sub>1-β</sub> and SnO<sub>2-γ</sub> [13]. However, SPPS is a process with ultra-high heating temperatures. In this work, we used low temperature process and we achieved NO<sub>2</sub> detection at temperatures not higher than 100°C to be compatible with most of flexible substrate aging. These detections have been made under UV activation by Al-ZnO NPs deposited on interdigitated electrodes fabricated on Si/SiO<sub>2</sub> substrate using photolithography. In Section II, the Al-ZnO solution process will be described and the results will be discussed in Section III.

## II. DESCRIPTION OF APPROACH AND TECHNIQUES

This description is composed of two parts, one is the sensing film fabrication; the other is the measurement system set-up.

### A. Al-ZnO solution

In order to maintain a cost efficient integration process, solution based materials are used as they show an outstanding tradeoff between cost and system complexity. The use of a nanoparticle dispersion of the ZnO semiconducting material doped by aluminum avoids most of the issues related to temperature. It is an attractive method

for the following reasons: good homogeneity, ease of composition control, and large area coatings with cost effective processes. Al-ZnO (or AZO) NPs were prepared following procedures described previously [14,15]. In a typical experiment, Al-ZnO NPs were produced by adding zinc acetate, aluminum isopropylate and distilled water into a flask containing anhydrous ethanol. After heating at 80°C, potassium hydroxide dispersed in ethanol was added dropwise to the flask, and heating was kept at 80°C during 16h. The as-synthesized Al-ZnO NPs were washed by centrifugation. By controlling the initial ratio of the aluminum to zinc precursor during synthesis while keeping constant all the other parameters, a precise control of Al doping content (atomic percentage, at.%) can be obtained. In the present study, Al-ZnO NPs with 0.8 at.% Al doping level have been synthesized. Size distribution of the NPs within the solutions was determined with Dynamic Light Scattering methods (DLS) using a NanoZetaSizer from Malvern. The solution-processable dispersions were prepared by transferring the synthesized Al-ZnO NPs from alcohol solutions to isopropanol at constant concentrations of 30 mg.mL<sup>-1</sup>. Additionally, cluster-free dispersion of Al-ZnO NPs was obtained in isopropanol by using 0.2 vol.% of ethanol amine (EA) as surfactant [14]. EA is a small organic molecule giving high dispersions in alcohols and avoiding the need of bulky or long surfactants.

Morphological study of Al-ZnO NPs was carried out by the high-resolution transmission electron microscope (HR-TEM) JEOL 3010, where samples were prepared by drop casting of diluted solution on a mesh-coated carbon film. Fig. 1 shows the EA-modified Al-ZnO NPs disperse in solution, which is not a complete translucent solution due to the Al doping. A typical Transmission Electron Microscopy (TEM) image of this Al-ZnO nanocrystals is shown on the right side of the Fig. 1, evidencing their size (diameter about 10 nm) and homogeneous size and shape dispersions.

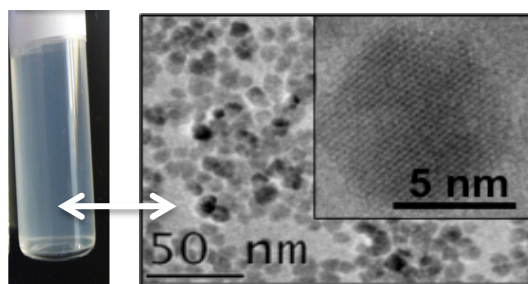


Figure 1. Optical image of solution based on Al-ZnO NPs in isopropanol (Al-ZnO NPs with 0.8 at.% of Al et 0.2 vol.% of EA) and TEM image of Al-ZnO nanocrystals drop-casted on a TEM grid [1].

Microstructure of thin films has been investigated using high-resolution scanning electron microscope (JEOL JSM 6320F). SEM micrographs were made on top sections on NPs-based thin films deposited on silicon substrates covered with 300 nm thick SiO<sub>2</sub> dielectric layers. In order to get details in microstructure of thin films, solutions containing NPs in isopropanol were deposited by spin-coating on SiO<sub>2</sub> substrates following by a thermal post-treatment at 150°C

for 30 min. With a boiling point (Tbp) of 82.6°C for isopropanol, solvent molecules were completely evaporated for annealing temperature reaching 150°C, but the EA surfactant molecules stayed adsorbed on the surface of NPs (Tbp = 170°C for EA) [16]. Previous analyses have shown that the Al-ZnO nanocrystals are monocrystalline with a classical wurtzite structure [14]. Starting from a dispersion state (i.e., the ink), the resulting solid states will depend not only on the chemical parameters of the materials but also on physical parameters such as deposition technique, substrate, drying process, thermal post-annealing, etc. The implementation and characterization of solution-processed gas sensors by drop casting or spin-coating require the thin film characterization. The morphological properties of the AZO thin films grown on SiO<sub>2</sub> substrates were examined by Scanning Electron Microscopy (SEM).

Fig. 2 shows SEM images of Al-ZnO thin films deposited by spin coating with a speed of 2000 rpm/min during 30 s.

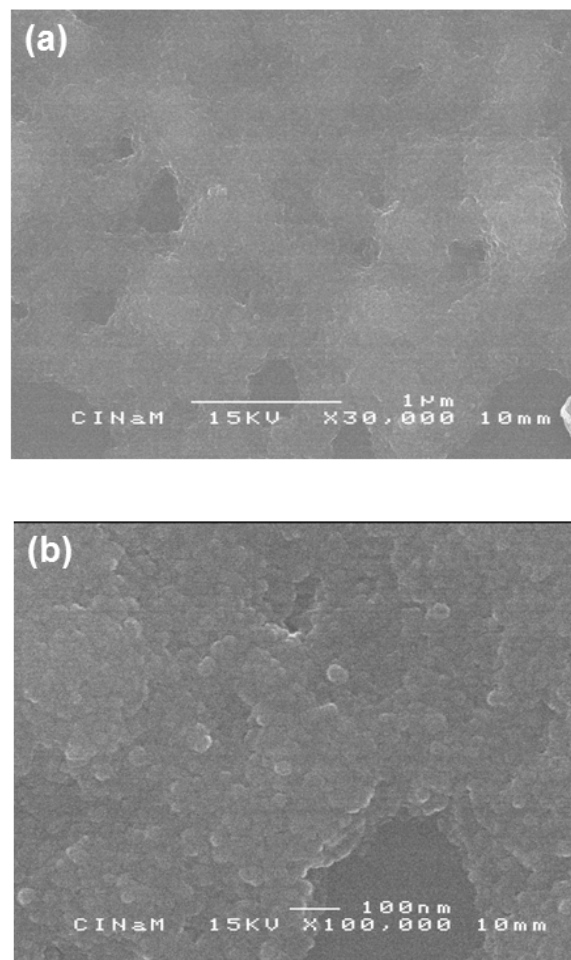


Figure 2. SEM images of Al-ZnO nanoparticles deposited on Si/SiO<sub>2</sub> substrates and heated at 150°C.

After the solution deposition, the coated substrates were annealed onto a preheated hotplate at 150°C for 30 min as a post-treatment in a nitrogen-filled glove box.

Fig. 2 shows the surface uniformity of Al-ZnO thin films on a large scale and a smaller scale. Small agglomerates, with a diameter of 15-25 nm, uniformly and densely dispersed on the surface were formed. By drop coating, Al-ZnO NPs entirely cover the substrate surface but with a less uniform morphology where the presence of tightly packed grains is observed. In both case, the free-spaces between NPs offer a high surface-area-to-volume-ratio to the thin film. Such surface structure gives a porous property to the thin films where gas molecules can diffuse in the volume structure.

### B. Gas sensors and set up

The gas sensing properties of Al-ZnO films were investigated in a sealed stainless test cell to control the substrate temperature and NO<sub>2</sub> concentrations. Our gas sensor consists of Ti/Pt interdigitated electrodes for gas detection. Temperature can be controlled underneath to improve the gas detection. The metal electrodes Ti/Pt were deposited on Si/SiO<sub>2</sub> by magnetron sputtering with thicknesses of 5 and 100 nm, respectively. In this work, Al-ZnO nanoparticles were deposited by drop coating. They were used as sensitive material with thickness of 200±10 nm measured by a Dektak 6M stylus profiler. The Al-ZnO films obtained were annealed for 30 min at 150°C for removing solvents and improving their quality and stability. The aim was to study the possible use, in a future work, on flexible substrates, which do not allow high temperature process. In order to find the best operating conditions, the gas sensing properties of Al-ZnO films were investigated in a sealed stainless test cell to control the substrate temperature and NO<sub>2</sub> concentrations. The measurements were made keeping in mind that the maximum NO<sub>2</sub> concentration is 100 ppb for 1h exposure and 75 ppb per day [17]. Dry air was used as both the reference and the carrier gas maintaining a constant total flow of 500 standard cubic centimeters per minute (SCCM) via mass flow controllers. The sensor was exposed to dry air (i.e. 0% relative humidity) with different concentrations of NO<sub>2</sub> (0.2, 0.5, 1, and 2 ppm) during 30 s and finally exposed to a clean dry airflow for recovery. The dry air and NO<sub>2</sub> gas were blown directly onto the sample placed on a heated holder. The applied DC voltage was 0.1 V. The electrical resistance was measured using a Keithley (model 2450) source-meter connected to a computer with a homemade program. Gas response of the sensor is defined by (1) as the ratio of the resistance change on the surface of the gas sensor before and after being exposed to NO<sub>2</sub>:

$$R = R_{\text{NO}_2} / R_{\text{dry air}} \quad (1)$$

where  $R_{\text{NO}_2}$  is the sensor resistance in presence of NO<sub>2</sub> and  $R_{\text{dry air}}$  is the sensor resistance through dry air flow.

The time exposure was fixed to 30s. Even if this time not allows reaching the sensor saturation, sufficient changes in resistance can be observed to extract information about the gas detection. The sensor response time is defined as the time required for a change in the sample's electrical resistance to reach 90% of the initial value when exposed to ozone gas. In the same way, the recovery time is defined as

the time required for the electrical resistance of the sensor to return 90% of the initial value after turning off the NO<sub>2</sub> gas. Several preliminary tests on conductivity change have been made using blue, red, UV, and green Light Emitted Diode (LED) under dry airflow without gas. The highest conductivity improvements have been obtained with UV LED. Gas sensing measurements under UV-light irradiation were performed using a UV-LED (Ref. UV5TZ-390-30 peak wavelength of 390 nm). Respectively, the blue LED (Ref. 247-1690, peak wavelength of 430 nm) was used with the same power than the UV one fixed at 60 mW. The distance between one LED and the sensing material is an important parameter. In our homemade test cell, this distance can be adjusted to obtain the higher conductivity under dry airflow than kept it constant during the gas detection. Measurement system pictures for testing gas sensors under UV light are given in Fig. 3.

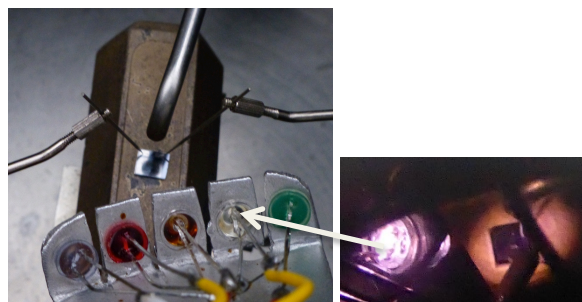


Figure 3. Experimental setup for gas sensors with Light Emitted Diode.

Before measurements, the sample was illuminated for 60 min with the chosen LED under dry air 500 SCCM, to stabilize the electrical resistance.

### III. RESULTS AND DISCUSSION

The gas sensor fabricated with Al-ZnO nanoparticles as sensitive material and deposited by drop coating on Si/SiO<sub>2</sub> substrate is presented in Fig. 4.

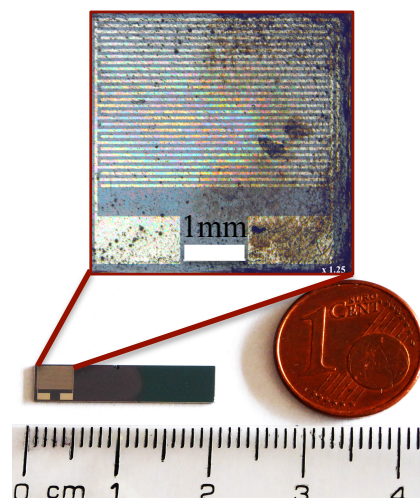


Figure 4. Sensor fabricated on Si/SiO<sub>2</sub> substrate.

The sample studied here was initially exposed to NO<sub>2</sub> at room temperature (at 25°C) without any illumination. As can be seen in Fig. 5, low resistance increases were observed without recovery. In the presence of gases, the electrical conductivity of semiconductor film sensor changes due to two main reactions occurring on the surface. The gas response is related to the number of oxygen ions adsorbed on the film surface. In n-type semiconductors, the majority charge carriers are electrons. When they are exposed to an oxidizing gas a decrease of conductivity occurs. After the gas is absorbed on the ZnO surface, the O atoms of oxidative gas molecules extract the electrons from the ZnO nanostructure; consequently, the depletion layer becomes thicker due to the decreasing of the carrier concentration [18].

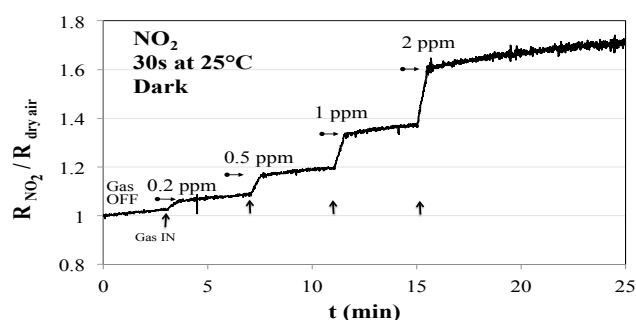


Figure 5. Sensor responses at 25°C in dark for 0.2 ppm to 2 ppm NO<sub>2</sub>.

At temperatures less than 150°C, the ionic species O<sub>2</sub> are dominant. These O<sub>2</sub> species contribute to form a high-resistance depletion layer in the NPs surfaces, increasing electrical resistance in the nanoparticles. Moreover, more oxygen vacancy related defects are introduced by Al doping, which increase the surface depletion thickness and the potential barrier height at the contact [19]. First, when the Al-ZnO NPs are exposed to an air atmosphere, oxygen molecules are adsorbed on the different surfaces. These oxygen molecules capture free electrons from the ZnO conduction band, forming ionized oxygen anions. Then, when Al-ZnO NPs gets exposed to NO<sub>2</sub> (a typical oxidizing gas), the NO<sub>2</sub> gas molecules adsorb on the Al-ZnO NPs surface, implying the formation of an electron-depletion layer due to adsorption of ions, which increases the potential barrier and diminishes Al-ZnO NPs conductivity. However, this last reaction needs enough energy to occur and the gas desorption is not possible at room temperature due to a lack of energy. When the NPs are exposed to UV irradiation (3.3 eV), electron-hole pairs are photogenerated ((e-) + (h+)) in the Al-ZnO NPs surface. The photogenerated holes (h+) could migrate to the Al-ZnO NPs surface, and O<sub>2</sub> species photodesorbed. As consequence, the depletion layer is diminished and the remaining unpaired electrons contribute to an increase in the electrical conductivity. Upon exposure to NO<sub>2</sub> gas, NO<sub>2</sub> molecules adsorb on the Al-ZnO NPs surfaces. This reaction widens the depletion-layer in the Al-ZnO NPs surface, and consequently, the electrical resistance is increased when the sensing material is exposed to NO<sub>2</sub>

gas, as shown in Fig. 5 at room temperature without humidity. Fig. 6 presents a comparison between the sensor responses without and with light illumination at room temperature for the NO<sub>2</sub> concentrations used in this work.

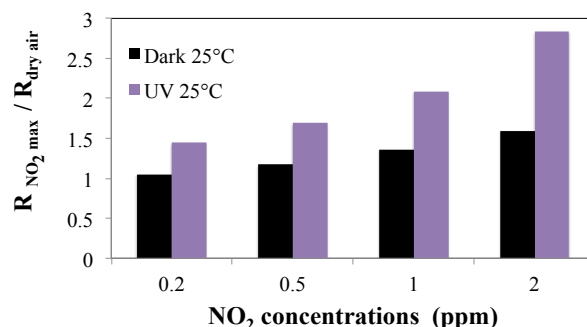


Figure 6. Comparison of sensor responses at 25°C in dark and under UV light at room temperature.

Under continuous UV illumination, the interaction between NO<sub>2</sub> and Al-ZnO NPs is enhanced over than without UV light due to the abundant photo generated free electrons.

The responses plotted in Fig. 7a at 25°C under UV light, demonstrate the total reversibility and good stability of the base line. However, about 45 minutes are needed to return to the baseline. The responses plotted in Fig. 7b at 25°C under a blue LED show great amplitude improvements but the return times were three times longer compare to the return times obtained under a UV LED.

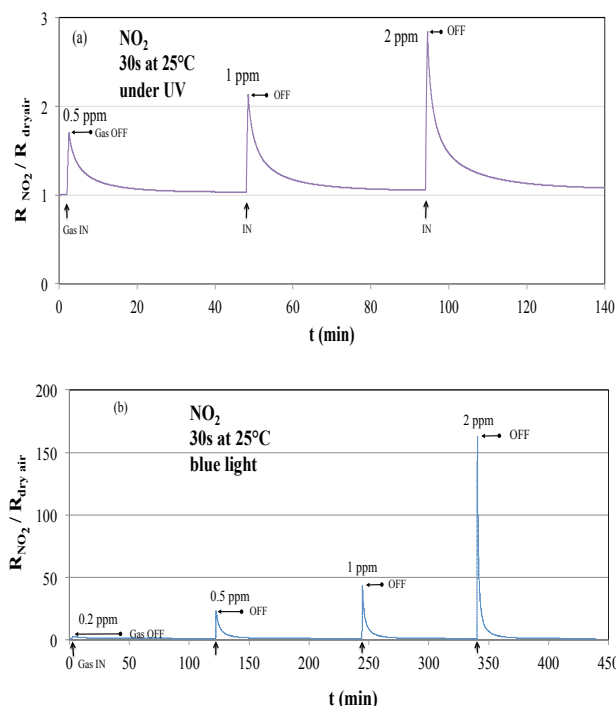


Figure 7. Sensor responses at 25°C for 0.5 ppm to 2 ppm NO<sub>2</sub> a) under a UV LED and b) under a blue LED.

Heating excitations were also tested up to 100°C in dark and under UV and blue illuminations. In dark, at 25°C and 50°C the resistance increases were observed without recovery. From 75°C in dark, the resistance returns to its reference value obtained through dry airflow for 1 and 2 ppm. At an operating temperature equals to 100°C the response is slightly higher than at 75°C, however, the recovery was observed for all concentrations. Fig. 8 shows responses in dark for 0.2 ppm to 2 ppm of NO<sub>2</sub> at 100°C. The response and the recovery time were improved by the heating excitation.

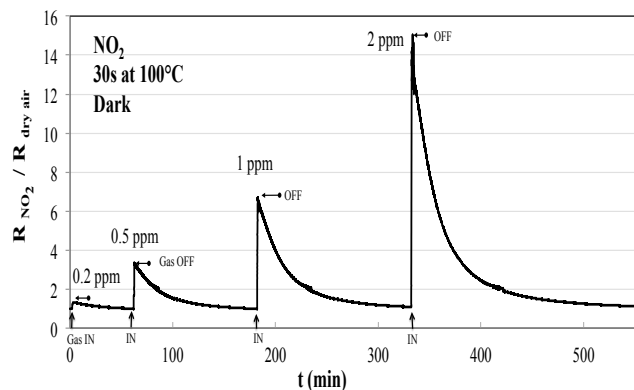


Figure 8. Sensor responses at 100°C in dark for 0.2 ppm to 2 ppm NO<sub>2</sub>.

To decrease the recovery time under light illuminations, temperature excitation is required. Indeed, the heating temperatures improve the chemical reactions at the sensitive surface layer. The response amplitudes were therefore enhanced for the four tested concentrations under UV light. Fig. 9a presents the best response in terms of amplitudes and recovery times obtained at 100°C under UV illumination for 0.2 ppm to 2 ppm of NO<sub>2</sub>. Fig. 9b highlights that the amplitude responses were greatly improved at 100°C by the blue light compare to the measurements performed in dark or under UV LED at this temperature. Nevertheless, the return times were around five times longer than the return times obtained under UV illumination.

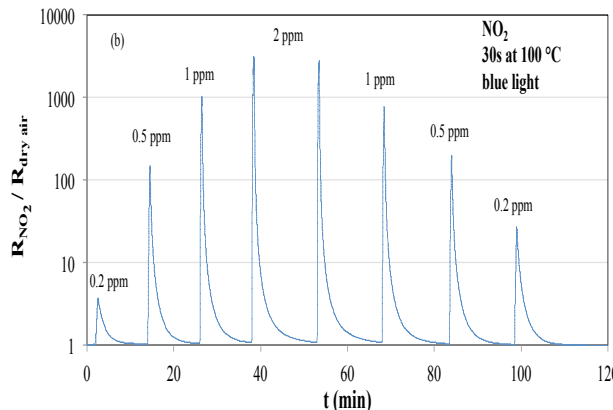
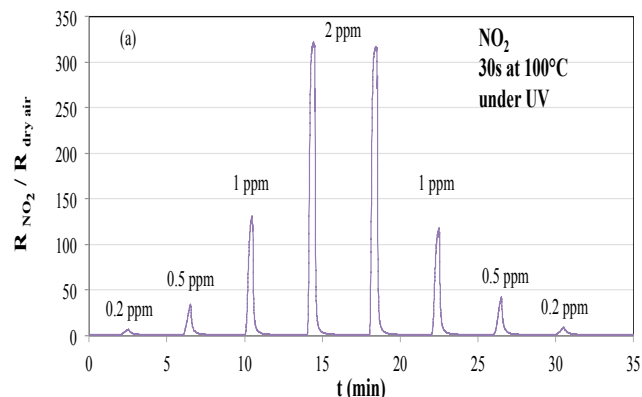


Figure 9. Sensor responses at 100°C for 0.2 to 2 ppm NO<sub>2</sub>: a) under a UV LED and b) under a blue LED.

Under UV illumination, the results obtained show fast response at low level of NO<sub>2</sub> concentration and good reversibility without sensor saturation. By increasing the temperature up to 100°C, the response amplitude for 2 ppm under the UV LEDt was multiplied by 200 at least and the time to return to the baseline was divided by 10.

Fig. 10 illustrates the good sensor response repeatability at 100°C under UV light illumination for 0.2 ppm of NO<sub>2</sub>.

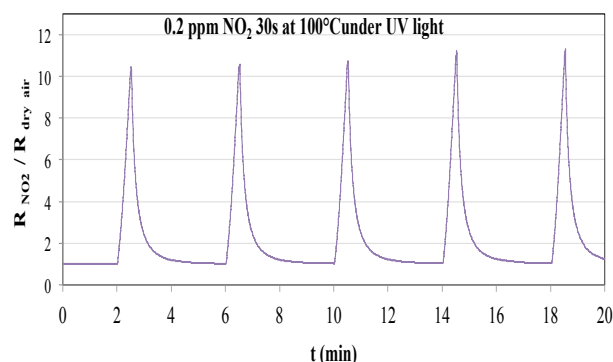


Figure 10. Response repeatability at 100°C under a UV LED for 0.2 ppm NO<sub>2</sub>.

#### IV. CONCLUSION

This paper reports nitrogen dioxide (NO<sub>2</sub>) detection at temperature up to 100°C. Room temperature NO<sub>2</sub> detection have been achieved by sensors on rigid substrate and improved with one UV Light Emitted Diode illumination. The gas measurements in our experiments under UV showed good responses with fast response and return times towards NO<sub>2</sub> even at 0.2 ppm. The photogenerated charge carriers (electrons and holes) present important benefits for working at low temperatures. UV light illumination results in an increase in the response signal, enhanced sensing reversibility, and an enhanced recovery rate at 100°C with good repeatability. It is open a new way to use Al-ZnO nanoparticles as sensitive layer for gas sensor devices on flexible substrates.

## ACKNOWLEDGMENT

The authors would like to thank A. Combes from IM2NP (UMR 7334) for his technical support in this work. The authors are grateful to D. Chaudansson from CINaM (UMR 7325) for assistance in TEM and SEM measurements.

## REFERENCES

- [1] S. Bernardini, B. Lawson, K. Aguir, O. Margeat, C. Videlot-Ackermann, and J. Ackermann, "Aluminum-doped zinc oxide nanocrystals for NO<sub>2</sub> detection at low temperature", *Allsensors 2017, The Second International Conference on Advances in Sensors, Actuators, Metering and Sensing*, pp. 56–57, March 2017, ISBN: 978-1-61208-543-2
- [2] T. Stubhan, I. Litzov, N. Li, M. Salinas,; M. Steidl, G. Sauer, et al., "Overcoming interface losses in organic solar cells by applying low temperature", *Solution Processed Aluminum-doped zinc oxide electron extraction layers*, *Journal of Materials Chemistry A* 2013, vol. 1, pp. 6004–6009, April 2013, doi:10.1039/c3ta10987a
- [3] M. Othman, D. Lollman, K. Aguir, P. Ménini, W. Belkacem, and N. Mliki, "Response enhancement of WO<sub>3</sub> gas sensors by metallic nanograins", *IEEE Sensors conference, Baltimore, SENSORS, 2013 IEEE, ISSN: 1930-0395, December 2013*, doi: 10.1109/icsens.2013.6688193
- [4] G.N. Chaudhari, A.M. Bende, A.B. Bodade, S.S. Patil, and V.S. Sapkal, "Structural and gas sensing properties of nanocrystalline TiO<sub>2</sub>:WO<sub>3</sub>-based hydrogen sensors", *Sensors and Actuators B: Chemical*, vol. 115, pp. 297–302, May 2006, doi: 10.1016/j.snb.2005.09.014
- [5] M. Ivanovskaya, D. Kotsikau, G. Faglia, P. Nelli, and S. Irkaev, "Gas sensitive properties of thin film heterojunction structures based on Fe<sub>2</sub>O<sub>3</sub>-In<sub>2</sub>O<sub>3</sub> nanocomposites", *Sensors and Actuators B: Chemical*, vol. 93, August 2003, pp. 422–430, doi:10.1016/S0925-4005(03)00175-8
- [6] E. Comini, A. Cristalli, G. Faglia, and G. Sberveglieri, "Light enhanced gas sensing properties of indium oxide and tin dioxide sensors", *Sensors and Actuators B: Chemical*, vol.65, pp. 260–263, June 2000, doi: 10.1016/S0925-4005(99)00350-0
- [7] E. Comini, G. Faglia, and G. Sberveglieri, "UV light activation of tin oxide thin films for NO<sub>2</sub> sensing at low temperatures", *Sensors and Actuators B: Chemical*, vol. 78, pp.73–77, August 2001, doi: 10.1016/S0925-4005(01)00796-1
- [8] L.B. Deng, X.H. Ding, D.W. Zeng, S.Q. Tian, H.Y. Li, and C.S. Xie, "Visible-light activate mesoporous WO<sub>3</sub> sensors with enhanced formaldehyde-sensing property at room temperature", *Sensors and Actuators B: Chemical*, vol. 163, pp. 260–266, March 2012, doi: 10.1016/j.snb.2012.01.049
- [9] B.P.J. de Lacy Costello, R.J. Ewen, N.M. Ratcliffe, and M. Richards, "Highly sensitive room temperature sensors on the UV-LED activation of zinc oxide nanoparticles", *Sensors and Actuators B: Chemical*, vol. 134, pp. 945–952, September 2008, doi: 10.1016/j.snb.2008.06.055
- [10] S.W. Fan, A.K. Srivastava, and V.P. Dravid, "UV-activated room-temperature gas sensing mechanism of polycrystalline ZnO", *Applied Physics Letters*, vol. 95, pp. 142106–142108, October 2009, doi: 10.1063/1.3243458
- [11] J.D.Prades, R. Jimenez-Diaz, F. Hernandez-Ramirez, S. Barth, A. Ciera, A. Romano-Rodriguez, et. al., "Equivalence between thermal and room temperature UV light-modulated responses of gas sensors based on individual SnO<sub>2</sub> Nanowires", *Sensors and Actuators B: Chemical*, vol. 140, pp. 337–341, July 2009, doi:10.1016/j.snb.2009.04.070
- [12] L. da Silva, J.C. M'Peko, A. C. Catto, S. Bernardini, V.R. Mastelaro, K. Aguir, et al., "UV-enhanced ozone gas sensing response of ZnO-SnO<sub>2</sub> heterojunctions at room temperature", *Sensors and Actuators B: Chemical*, vol. 240, pp. 573–579, March 2017, doi: 10.1016/j.snb.2016.08.158
- [13] Xin Geng, Chao Zhang, Yifan Luoa, Hanlin Liaod, Marc Debliquy "Light assisted room-temperature NO<sub>2</sub> sensors with enhanced performance based on black SnO<sub>1-α</sub>@ZnO<sub>1-β</sub>@SnO<sub>2-γ</sub> nanocomposite coatings deposited by solution precursor plasma spray", *Ceramics International*, vol. 43 pp. 5990–5998, January 2017, doi: 10.1016/j.ceramint.2017.01.136
- [14] M. Gaceur, S. Ben Dkhil, D. Duché, F. Bencheikh, JJ. Simon, L. Escoubas, et al. , "Ligand-free synthesis of aluminium-doped zinc oxide nanocrystals and their use as optical spacers in color-tuned highly efficient organic solar cells", *Advanced Functional Materials*, vol. 26, pp. 243–253, January 2016, doi:10.1002/adfm.201502929
- [15] A.K. Diallo, M. Gaceur, S. Fall, Y. Didane, S. Ben Dkhil, O. Margeat, et al. , "Insight about electrical properties of low-temperature solution-processed Al-doped ZnO nanoparticle based layers for TFT applications". *Materials Science and Engineering: B*, vol. 214, pp. 11–18, July 2016, doi: 10.1016/j.mseb.2016.07.015
- [16] A.K. Diallo, M. Gaceur, S. Ben Dkhil, Y. Didane, O. Margeat, J. Ackermann, et al. , "Impact of surfactants covering ZnO nanoparticles on solution-processed field-effect transistors: from dispersion state to solid state". *Colloids and Surfaces A*, vol. 500, pp. 214–221, April 2016, doi: 10.1016/j.colsurfa.2016.04.036
- [17] WHO guidelines for NO<sub>2</sub>, <http://www.who.int/mediacentre/factsheets/fs313/en/>
- [18] M. Acuaatla, S. Bernardini, L. Gallais, T. Fiorido, L. Pattout, and M. Bendahan, "Ozone flexible sensors fabricated by photolithography and laser ablation processes based on ZnO nanoparticles", *Sensors and Actuators B: Chemical* vol. 203, pp: 602–611, November 2014, doi: 10.1016/j.snb.2014.07.010
- [19] T.A. Moore, I.M. Miron, G. Gaudin, G. Serret, S. Auffret, B. Rodmacq, et al. , "High domain wall velocities induced by current in ultrathin Pt/Co/AlOx wires with perpendicular magnetic anisotropy", *Applied Physics Letters*, vol. 93, pp. 263103–263103-3, January 2009, doi: 10.1063/1.3062855.